

Diffusion-weighted magnetic resonance imaging of thymoma: ability of the Apparent Diffusion Coefficient in predicting the World Health Organization (WHO) classification and the Masaoka-Koga staging system and its prognostic significance on disease-free survival

Adriano Massimiliano Priola¹ · Sandro Massimo Priola¹ · Maria Teresa Giraudo⁴ · Dario Gned¹ · Alessandro Fornari² · Bruno Ferrero³ · Lorena Ducco¹ · Andrea Veltri¹

Received: 19 June 2015 / Accepted: 15 September 2015 / Published online: 1 October 2015
© European Society of Radiology 2015

Abstract

Objectives To evaluate the usefulness of diffusion-weighted magnetic resonance for distinguishing thymomas according to WHO and Masaoka-Koga classifications and in predicting disease-free survival (DFS) by using the apparent diffusion coefficient (ADC).

Methods Forty-one patients were grouped based on WHO (low-risk vs. high-risk) and Masaoka-Koga (early vs. advanced) classifications. For prognosis, seven patients with recurrence at follow-up were grouped separately from healthy subjects. Differences on ADC levels between groups were tested using Student-*t* testing. Logistic regression models and areas under the ROC curve (AUROC) were estimated.

Results Mean ADC values were different between groups of WHO (low-risk= $1.58 \pm 0.20 \times 10^{-3} \text{ mm}^2/\text{sec}$; high-risk= $1.21 \pm 0.23 \times 10^{-3} \text{ mm}^2/\text{sec}$; $p < 0.0001$) and Masaoka-Koga (early= $1.43 \pm 0.26 \times 10^{-3} \text{ mm}^2/\text{sec}$; advanced= $1.31 \pm 0.31 \times 10^{-3} \text{ mm}^2/\text{sec}$; $p = 0.016$) classifications. Mean ADC of type-B3 ($1.05 \pm$

$0.17 \times 10^{-3} \text{ mm}^2/\text{sec}$) was lower than type-B2 ($1.32 \pm 0.20 \times 10^{-3} \text{ mm}^2/\text{sec}$; $p = 0.023$). AUROC in discriminating groups was 0.864 for WHO classification (cut-point= $1.309 \times 10^{-3} \text{ mm}^2/\text{sec}$; accuracy=78.1 %) and 0.730 for Masaoka-Koga classification (cut-point= $1.243 \times 10^{-3} \text{ mm}^2/\text{sec}$; accuracy=73.2 %). Logistic regression models and two-way ANOVA were significant for WHO classification (odds ratio[OR]=0.93, $p = 0.007$; $p < 0.001$), but not for Masaoka-Koga classification (OR=0.98, $p = 0.31$; $p = 0.38$). ADC levels were significantly associated with DFS recurrence rate being higher for patients with $\text{ADC} \leq 1.299 \times 10^{-3} \text{ mm}^2/\text{sec}$ ($p = 0.001$; AUROC, 0.834; accuracy=78.0 %).

Conclusions ADC helps to differentiate high-risk from low-risk thymomas and discriminates the more aggressive type-B3. Primary tumour ADC is a prognostic indicator of recurrence.

Key Points

- DW-MRI is useful in characterizing thymomas and in predicting disease-free survival.
- ADC can differentiate low-risk from high-risk thymomas based on different histological composition
- The cutoff-ADC-value of $1.309 \times 10^{-3} \text{ mm}^2/\text{sec}$ is proposed as optimal cut-point for this differentiation
- The ADC ability in predicting Masaoka-Koga stage is uncertain and needs further validations
- ADC has prognostic value on disease-free survival and helps in stratification of risk

Keywords Thymoma · WHO classification · Masaoka-Koga staging system · Diffusion-weighted magnetic resonance imaging · Apparent diffusion coefficient

✉ Adriano Massimiliano Priola
adriano.priola@inwind.it

¹ Department of Diagnostic Imaging, San Luigi Gonzaga University Hospital, Regione Gonzole 10, 10043 Orbassano (Torino), Italy

² Department of Pathology, San Luigi Gonzaga University Hospital, Regione Gonzole 10, 10043 Orbassano (Torino), Italy

³ Department of Neurology, San Luigi Gonzaga University Hospital, Regione Gonzole 10, 10043 Orbassano (Torino), Italy

⁴ Department of Mathematics “Giuseppe Peano”, University of Torino, Via Carlo Alberto 10, 10123 Torino, Italy

Introduction

Thymomas are benign or low-grade malignant tumours of the thymic epithelium and represent up to half of all neoplasms of the anterior mediastinum [1–6]. The histological classification proposed by the World Health Organization (WHO) and the Masaoka-Koga staging system, based on surgical findings, is currently used for treatment planning and significantly correlate with prognosis [1–8]. The Jeong simplification of WHO classification includes low-risk thymomas, high-risk thymomas, and thymic carcinomas [9]. The Masaoka-Koga system includes early (stage I–II) and advanced thymomas (stage III–IV) [8]. The correct prediction of early or advanced disease before surgery at imaging is essential to plan treatment strategies, because the latter receives neo-adjuvant chemotherapy [2]. Unfortunately, there is no perfect correlation among Jeong and Masaoka-Koga classifications because, although low-risk thymomas are frequently grouped in the early-disease group, percentages of high-risk thymomas are reported at a rate up to 45 % in the early stage disease group [10].

Limited data are available on quantitative assessment of thymic epithelial tumours (TETs) by using diffusion-weighted magnetic resonance imaging (DW-MRI) from small cohorts of studies which considered various anterior mediastinal tumours, although those studies did not attempt to differentiate thymomas based on WHO and Masaoka-Koga classifications by using the ADC [11–18]. More recently, a study involving 30 patients with TETs has demonstrated the ability of ADC in differentiating low-risk from high-risk tumours, and early from advanced disease [19]. Despite such promising results, that study is influenced by a strong correlation between Jeong and Masaoka-Koga classifications and by the inclusion of thymic carcinomas in the advanced disease group which leads to further decrease of the mean ADC value of this group compared with the early disease group [19, 20]. Moreover, perfusion-sensitive ADC values have been used for analyses by including the b value of 0 sec/mm² for ADC computation, obtaining a measured signal which reflects not only pure molecular water diffusion, but also “pseudo-diffusion” resulting from fast-moving water molecules from blood flow in vessels and capillaries [21–25]. Hence, the ability of DW-MRI in distinguishing thymomas based on WHO and Masaoka-Koga classifications remains uncertain and optimal ADC cut-points should be validated.

To date, no study has evaluated the predictive value of ADC of thymomas on disease-free survival (DFS) of patients with a thymoma for optimizing clinical decision making at diagnosis and improving patient care, although it is used as independent predictor of DFS and overall survival in different organs [23–25].

The aim of our study was to investigate the reliability of DW-MRI in predicting histological types of thymomas according to WHO classification, and whether DW-MRI can

differentiate low-risk from high-risk thymomas, and early from advanced disease by using perfusion-free ADC measurements, with proposed optimal cut-point values for each differentiation. Moreover, we evaluated the prognostic value of ADC of a primary tumour for predicting DFS.

Materials and methods

Patient population, reference diagnosis and patient outcome

From March 2007 through December 2014, 41 consecutive subjects [19 men, 22 women; all subjects: age range 28–80 ys, mean age \pm standard deviation (SD) 56.9 ys \pm 14.0 ys; male: 38–80 ys, 57.8 ys \pm 13.3 ys; female: 28–80 ys, 56.2 ys \pm 14.7 ys), who underwent thymomectomy and no neo-adjuvant treatments, were evaluated with MRI. Institutional review board approval was obtained and data were prospectively assessed.

The histopathologic results from surgical specimens were the standard of reference for each case classified based on WHO histological classification, simplified WHO classification proposed by Jeong, and the Masaoka-Koga staging system [7–9]. Tables 1 and 2 report definitions for both classifications with corresponding sample size.

For analyzing prognosis, recurrent disease was defined as evidence of local, regional, or distant disease determined by follow-up imaging and confirmed by biopsy. DFS was determined as the time interval between the date of surgery and date of documented disease recurrence or last follow-up for subjects with no recurrence. No deaths related to tumour occurred during the observational period, thus, no analysis on overall-survival was performed.

MRI protocol

DW-MRI was performed on a 1.5-Tesla (T) unit (Intera-Achieva, Philips Healthcare, Best, The Netherlands) using a single-shot spin-echo/echo-planar sequence with the following parameters: 360–500 mm field of view, 116 \times 224 image matrix, 45 echo planar imaging factor, 5-mm slice thickness, 0.5-mm intersection gap, 4500-msec repetition time, 62-msec echo time, 1600-Hz/pixel bandwidth. Four signals were acquired per image with diffusion sensitizing gradients applied in three orthogonal planes with b values of 0, 150, 500, and 800 sec/mm². All sequences were performed using a parallel imaging acquisition technique and sensitivity encoding reconstruction (reduction factor, 2). Fat was suppressed by placing a frequency-selective radiofrequency pulse before the pulse sequence.

Table 1 World Health Organization (WHO) histological classification of thymic epithelial tumours (2004)*

Type	Definition	No.
A	Spindle cells: bland spindle/oval epithelial tumour cells with few or no lymphocytes	3
AB	Mixed spindle cells and lymphocytes: mixture of a lymphocyte-poor type A thymoma component and a more lymphocyte-rich type B-like component	10
B1	Lymphocytes > epithelial cells, predominantly cortical: areas resembling cortex of the normal thymus with epithelial cells scattered in a prominent population of immature lymphocytes and areas of medullary differentiation with or without Hassall's corpuscles, similar to the normal thymic medulla. Some epithelial tumour cells present large nuclei of pale chromatin and small nucleoli	6
B2	Mixed lymphocytes and epithelial cells, cortical: large, polygonal tumour cells arranged in a loose network with large vascular nuclei and prominent large nucleoli, closely resembling the predominant epithelial cells of the normal thymic cortex. A background population of immature T cells is always detectable and lymphocytes are less abundant than in type B1	13
B3	Predominance of epithelial cells: prominent population of medium-sized round or polygonal epithelial cells with slight nuclear atypia and some prominent nucleoli mixed with a minor component of lymphocytes	9

No. = number of patients

Jeong modification = Type A, AB, B1: low-risk thymomas (19 patients); type B2, B3: high-risk thymomas (22 patients)

* From Müller-Hermelink et al. [7], modified

For each case, the entire lesion was included in the MRI. The mean time between MRI and surgery was 10 days (range, 1–21 days).

MR image analysis

All exams were evaluated independently by two radiologists (A.M.P., D.G.) who were blinded to the patients' identifications and clinical data. The longest thymoma diameter was measured at the widest dimension on transverse cross-sectional images. For quantitative assessment, ADC maps were reconstructed after excluding the *b* value of 0 sec/mm² to suppress tissue perfusion for obtaining perfusion-free ADC values by eliminating vascular contributions to the calculated ADC which would increase the ADC value [21–25]. For each case, within axial sections which included the tumour on ADC maps, a region of interest (ROI) was manually drawn along the circumference of the tumour, but within boundaries, to include only the solid portion of tissue, taking care to exclude obvious cystic and/or necrotic areas (which could give falsely

elevated ADC values) that were identified on corresponding T2-weighted images. The mean ADC was calculated from all values obtained for each case.

Statistical analysis

Categorical parameters and continuous numeric data with a normal distribution of demographic characteristics and imaging findings were compared between defined groups of each classification by using the Fisher's exact test and a Student's *t*-test, respectively. Data concerning ADC levels were expressed as mean values ± the standard deviation (SD) and ranges, because of their normal distributions proved by the Shapiro-Wilk test. The inter-reader agreement of ADC measurements was evaluated between readers by using the intra-class correlation coefficient (ICC, range: 0–1). The ADC levels were compared between defined groups of each classification (Jeong and Masaoka-Koga) and differences in mean values were analyzed using the Student's *t*-test. Moreover, for WHO classification, differences in the mean ADC value of

Table 2 Masaoka-Koga staging system for thymoma*

Stage	Definition	No.
I	Macroscopically completely encapsulated tumour, with no microscopically detectable capsular invasion	9
IIa	Macroscopic invasion into surrounding mediastinal fatty tissue or mediastinal pleura	7
IIb	Microscopic invasion into the capsule	8
III	Macroscopic invasion into neighbouring organs such as pericardium, great vessels, and lung	13
IVa	Pleural or pericardial dissemination through direct extension or drop metastasis	3
IVb	Lymphogeneous or haematogeneous metastases	1

No. = number of patients

Stage I–II: early thymoma (24 patients); stages III–IV: advanced thymoma (17 patients)

* From Masaoka et al. [8], modified

Table 3 Demographic characteristics and imaging findings of the 41 enrolled patients

Characteristic	Thymoma					
	WHO*			Masaoka-Koga		
	Low-risk	High-risk	<i>p</i>	Early	Advanced	<i>p</i>
Mean age (years) ± standard deviation (range)	63.1±12.4 (38–80)	51.6±13.3 (28–71)	.006	61.9±12.0 (38–80)	49.8±13.7 (28–74)	.006
Male/Female ratio	9/10	10/12	.990	13/11	9/8	.990
Mean size (mm) ± standard deviation (range)	39.3±12.0 (18–71)	56.9±22.2 (31–112)	.003	40.6±13.2 (18–77)	60.3±22.7 (34–112)	.004
Necrosis/Cystic areas Yes/No	2/17	8/14	.075	3/21	7/10	.063

Number of patients: low-risk, 19; high-risk, 22; early, 24; advanced, 17.

Size is the maximal diameter of the lesion, measured on transverse images.

Necrosis/Cystic areas refer to MR findings on T2-weighted imaging.

* Jeong simplification of WHO classification [9].

each histological type were assessed by using one-way analysis of variance (ANOVA) with multiple comparisons of means. Logistic regression models were estimated for evaluating the ability of ADC levels to discriminate between defined groups of Jeong and Masaoka-Koga classifications. Discrimination abilities were evaluated by the area under the receiver operating characteristic curve (AUROC) and optimal cut-points were determined according to the Youden index with computation of diagnostic accuracy. For WHO classification, AUROC with optimal cut-point and relative diagnostic accuracy were also estimated to assess the ability of ADC to differentiate type-B3 from other histological types. Additional analyses aimed to control for potential confounding factors (age, gender, lesion size) were performed for both classifications by including such factors in logistic regression models. The two-way ANOVA was used to examine the influence of defined groups of Jeong and Masaoka-Koga classifications together with their interaction. Lastly, the Cramér’s V (range: 0–1) was estimated to assess the association between Jeong and Masaoka-Koga classifications in our cohort. Considering DFS, the mean ADC levels were compared between two groups divided into subjects with and without recurrence at last follow-up by using the Student’s *t*-test. The ROC curve analysis was used to determine optimal cut-point values of

individual prognostic factors for DFS (age, gender, lesion size, resection status, WHO type, Masaoka-Koga stage, ADC), with computation of AUROC and diagnostic accuracy. Prognostic factors were analyzed by univariate analysis using the Kaplan-Meier method for estimation of DFS rates and differences between DFS curves, obtained by using the optimal cut-point for risk stratification of recurrence, were analyzed by the log-rank test. Multivariate analysis of prognostic factors was performed using the Cox proportional hazards regression model by including significant parameters obtained from univariate analysis in order to estimate the overall effect of ADC levels on DFS for ascertaining the independent prognostic value of ADC. A *p*<0.05 was considered indicative of a statistically significant difference. All analyses were performed with “R” and MedCalc software.

Results

Demographic data and imaging findings at conventional MRI

Demographic characteristics and imaging findings of patients and sample size of defined groups are detailed in

Table 4 Correlation between WHO histological classification and Masaoka-Koga staging system

WHO*	Masaoka-Koga			
	I (9)	II (15)	III (13)	IV (4)
Low-risk (A, AB, B1)	7 (0, 4, 3)	9 (3, 4, 2)	3 (0, 2, 1)	0
High-risk (B2, B3)	2 (2, 0)	6 (4, 2)	10 (5, 5)	4 (2, 2)

Numbers in parentheses are the number of patients

* Jeong simplification of WHO classification [9].

Table 5 Mean ADC values of thymomas according to WHO histological classification

WHO type	No. of patients	Mean ADC (× 10 ⁻³ mm ² s ⁻¹) ± standard deviation (range)
A	3	1.61±0.13 (1.50/1.76)
AB	10	1.62±0.22 (1.35/2.01)
B1	6	1.51±0.21 (1.24/1.80)
B2	13	1.32±0.20 (1.13/1.76)
B3	9	1.05±0.17 (0.73/1.38)

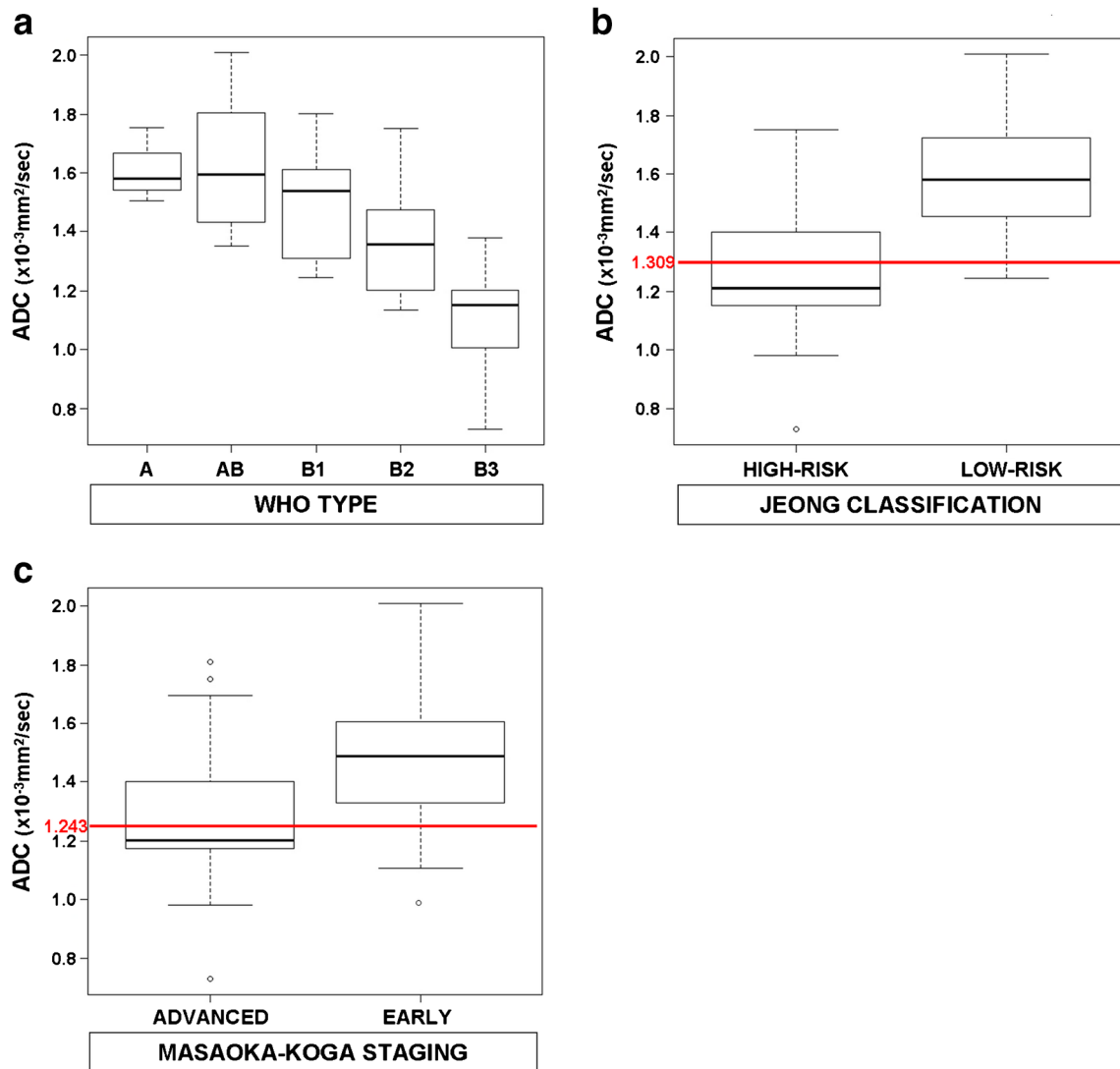


Fig. 1 Box-and-whiskers plots show ADC values for all cases divided into groups according to the WHO classification (**a**), the Jeong simplification of WHO classification (**b**), and the Masaoka-Koga staging system (**c**). The boxes represent data from the 25th to the 75th percentile. The horizontal line inside the boxes is the median (50th percentile). The vertical lines with whiskers indicate the range from the largest to smallest observed data point, within $1.5 \times \text{IQR}$ of the higher and lower quartile, respectively. The values outside this range (**b**, high-risk; **c**,

advanced and early) are displayed as individual points. The continuous horizontal red line in the graphs shows the optimal cut-point value for discrimination among defined groups deriving from the ROC analysis. Considering the Jeong and Masaoka-Koga classifications, a larger overlap zone is appreciable for Masaoka-Koga staging system (from 0.99 to $1.81 \times 10^{-3} \text{ mm}^2/\text{sec}$) compared with Jeong classification (from 1.24 to $1.75 \times 10^{-3} \text{ mm}^2/\text{sec}$)

Table 3. For both classifications, there was a significant difference in mean age and size of tumours in the low-risk and early-disease group compared with those in the high-risk and advanced-disease group, respectively.

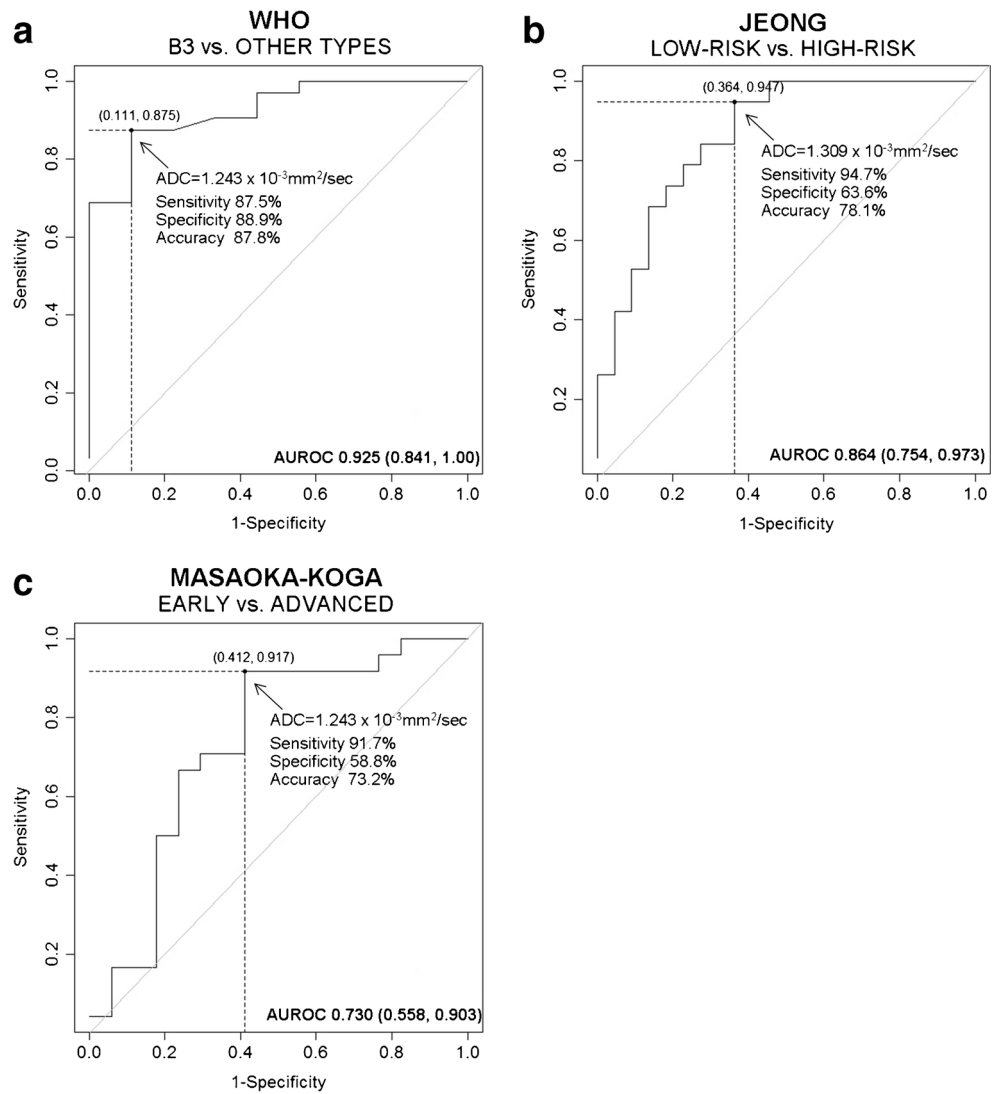
Table 4 reports the relation between Jeong classification and Masaoka-Koga staging. Low-risk thymomas were mostly classified in the early-disease group (16/19, 84.2 %), whereas only 15.8 % (3/19) of cases were defined as advanced disease. Conversely, a substantial percentage of high-risk thymomas were grouped in the early-disease group (8/22, 36.4 %) with the remaining 63.6 % (14/22) of high-risk thymomas in the advanced-

disease group. The estimation of Cramér's index ($V=0.518$) indicated a mild association between Jeong and Masaoka-Koga classifications in our cohort.

Inter-reader variability for ADC measurements

For ADC measurements, the inter-reader agreement was high with an ICC of 0.885 (95 % confidence interval [95 % CI]: 0.842–0.911). Therefore, for each case, the mean ADC value of readers was used for further analyses.

Fig. 2 Receiver operating characteristic (ROC) curves indicate the sensitivity, specificity, and diagnostic accuracy of ADC-based differentiation between the defined groups according to the WHO classification (**a**, B3 vs. all other types), the Jeong simplification of the WHO classification (**b**, low-risk vs. high-risk), and the Masaoka-Koga staging system (**c**, early vs. advanced). For each curve, the optimal cut-off value is highlighted with the relative values of sensitivity, specificity, and diagnostic accuracy



WHO classification: differences in ADC between histological types

Table 5 and Fig. 1a report ADC values and box plots of each histological type of thymoma according to WHO classification. The higher mean and maximum ADC values were found for type-AB (1.62 ± 0.22 and 2.01×10^{-3} mm/sec, respectively), whereas the lower mean and minimum ADC values were

found for type-B3 (1.05 ± 0.17 and 0.73×10^{-3} mm/sec, respectively). The one-way ANOVA demonstrated that ADC of type-B3 was significantly lower compared with all other types (B3 vs. B2, $p=0.023$; B3 vs. B1, $p=0.003$; B3 vs. AB, $p<0.0001$; B3 vs. A, $p=0.0003$). Contrariwise, no significant differences in mean ADC values were found between the other types, except for type-B2 compared with type-AB ($p=0.004$).

Table 6 Mean ADC values of low-risk versus high-risk and early versus advanced thymoma

Parameter	Thymoma		<i>p</i>
Mean ADC ($\times 10^{-3}$ mm ² /sec) \pm standard deviation (range)	Low-risk [19]	High-risk [22]	<0.0001
	1.58 \pm 0.20 (1.24/2.01)	1.21 \pm 0.23 (0.73/1.75)	
Mean ADC ($\times 10^{-3}$ mm ² /sec) \pm standard deviation (range)	Early [24]	Advanced [17]	0.016
	1.43 \pm 0.26 (0.99/2.01)	1.31 \pm 0.31 (0.73/1.81)	

Numbers in parentheses are the number of patients.

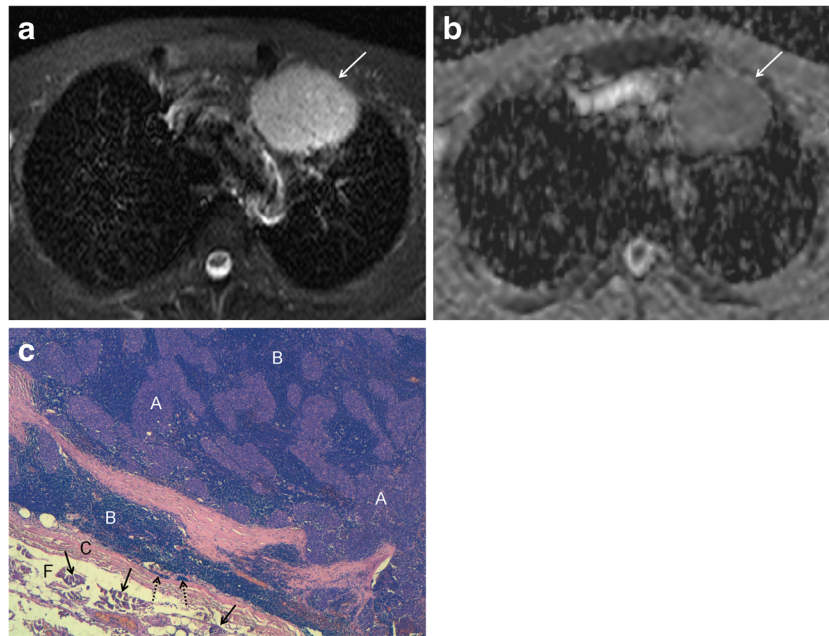


Fig. 3 Low-risk and early thymoma in a 56-year-old woman (WHO type AB, Masaoka-Koga stage II). **a** Transverse T2-weighted fat-suppressed MR image shows a soft tissue mass (arrow; maximal diameter, 59 mm) in the left side of the anterior mediastinum, adjacent to the aortic arch, with well defined borders and slightly heterogeneous high signal intensity. **b** The ADC map of DW-MRI demonstrates grey appearance of the mass (arrow), similar to that of muscles, with a mean ADC of 1.473×10^{-3} mm²/sec (standard deviation, 0.184; minimum and maximum value, 1.037 and 1.851×10^{-3} mm²/sec, respectively). **c** Photomicrograph of a

representative histological section detects tissue of high cellular density characterized by a mixed composition of pale lymphocyte-poor areas with spindle cell morphology (A, WHO type A component) and dark lymphocyte-rich areas (B, WHO type B component). The tumour is encapsulated (C, capsule) although microscopic invasion by small clusters of tumour cells is appreciable into the thin capsule (dotted arrows) and into the surrounding mediastinal fatty tissue (arrows; F, mediastinal fat; haematoxylin and eosin stain, original magnification $\times 40$)

The AUROC of ADC in discriminating B3 from all other types was 0.925 (95 % CI: 0.841–1.000; Fig. 2a). The optimal cut-point was identified as an ADC of 1.243×10^{-3} mm²/sec (Youden index $J=0.764$). Applying this cut-point for the identification of types other than B3, sensitivity was 87.5 % (28/32; 95 % CI: 71.9–95.0), specificity was 88.9 % (8/9; 95 % CI: 56.5–98.0), and accuracy was 87.8 % (36/41; 95 % CI: 74.5–94.7).

Jeong classification: differences in ADC between groups (low-risk vs. high-risk)

The mean ADC was significantly different between groups (1.58 and 1.21×10^{-3} mm²/sec, respectively, $p < 0.0001$; Table 6; Figs. 3 and 4). Figure 1b shows the box plots comparing the ADC values for the low-risk and high-risk groups.

Considering the logistic regression model for the groups, the probability of finding high-risk thymoma decreased with the increase of ADC [odds Ratio (OR) per 0.01 increase, 0.928; 95 % CI: 0.879–0.965; $p=0.001$]. The AUROC of ADC in discriminating between groups was 0.864 (95 % CI: 0.754–0.973; Fig. 2b). The optimal cut-point was identified as an ADC of 1.309×10^{-3} mm²/sec (Youden Index $J=0.584$). Applying this cut-point for the diagnosis of low-risk thymoma, the sensitivity was 94.7 % (18/19; 95 % CI: 75.4–99.1), specificity was 63.6 % (14/22; 95 % CI: 43.0–80.3),

and accuracy was 78.1 % (32/41; 95 % CI: 63.3–88.0). In the adjusted model, the OR was 0.930 per an ADC increase of 0.01 (95 % CI: 0.873–0.973; $p=0.007$).

Masaoka-Koga classification: differences in ADC between groups (early vs. advanced)

The mean ADC differed significantly between groups (1.43 and 1.31×10^{-3} mm²/sec, respectively, $p=0.016$; Table 6; Figs. 3 and 4). Figure 1c shows the box plots comparing the ADC values for the early and advanced group.

Considering the crude logistic regression model for the groups, the probability of finding advanced disease decreased with the increase of ADC (OR per 0.01 increase, 0.960; 95 % CI: 0.932–0.992; $p=0.02$). The AUROC of ADC in discriminating between groups was 0.730 (95 % CI: 0.558–0.903; Fig. 2c). The optimal cut-point was identified as an ADC of 1.243×10^{-3} mm²/sec (Youden index $J=0.505$). Applying this cut-point for the diagnosis of early thymoma, sensitivity was 91.7 % (22/24; 95 % CI: 74.2–97.7), specificity was 58.8 % (10/17; 95 % CI: 36.0–78.4), and accuracy was 73.2 % (30/41; 95 % CI: 59.4–87.0). In the adjusted model, the OR was 0.98 per 0.01 ADC increase but it did not yield statistical significance ($p=0.31$), as was the case for the two-way ANOVA ($p=0.38$).

Lastly, considering low-risk thymomas, there was insignificant difference between the mean ADC of low-risk thymomas classified in the early-disease and advanced-disease group (early: 13 cases, $1.55 \pm 0.22 \times 10^{-3}$ mm²/sec; advanced: 3 cases, $1.67 \pm 0.16 \times 10^{-3}$ mm²/sec; $p=0.42$). Similarly, for high-risk thymomas, there was no significant difference in mean ADC among the advanced-disease and early-disease groups (advanced: 14 cases, $1.23 \pm 0.27 \times 10^{-3}$ mm²/sec; early: 8 cases, $1.17 \pm 0.13 \times 10^{-3}$ mm²/sec; $p=0.56$; Figs. 4 and 5). Furthermore, there was no difference in mean ADC among type-B2 thymomas assigned in the early and advanced groups ($p=0.08$), as was the case among type-B3 thymomas ($p=0.95$).

Patient outcome and DFS analysis

Follow-up ranged from 6 to 94 months (median, 36 months) and seven subjects (17.1 %, 7/41) had recurrent disease (median, 22 months; range, 12–51 months; Table 7). DFS rates at last follow-up for the low-risk and early-disease group were 94.7 % (18/19) and 91.7 % (22/24), respectively, whereas those for the high-risk and advanced-disease group were 72.7 % (16/22) and 70.6 % (12/17), respectively.

Optimal ADC cut-point for group discrimination (recurrence vs. disease free) was determined using ROC analysis in ADC of 1.299×10^{-3} mm²/sec (Youden Index $J=0.622$;

AUROC=0.834). Applying this cut-point, for prediction of recurrence, sensitivity was 85.7 % (6/7; 95 %CI:0.744–0.964), specificity was 76.5 % (26/34; 95 %CI:0.631–0.897), and accuracy was 78.0 % (32/41; 95 %CI: 0.651–0.909; Fig. 6). By using the optimal cut-point as dichotomization threshold for Kaplan-Meier survival analysis, the group with lower ADC was found to have poorer DFS compared with the group with higher ADC (57.1 % [8/14] vs. 96.3 % [26/27]; $p=0.001$; Fig. 7). At univariate analysis, ADC was found to be significant prognostic factor (hazard ratio [HR]=0.959; 95 %CI: 0.931–0.988; $p<0.01$). Furthermore, at Kaplan-Meier analysis, lesion size and resection status were other factors significantly related with DFS ($p=0.007$ and 0.041, respectively; Table 8). At multivariate analysis performed with significant factors by using Cox proportional hazards regression, ADC was confirmed as significant independent prognostic factor (HR=0.969; 95 %CI: 0.939–0.999; $p=0.02$) with a significant overall model fit ($p=0.02$).

Discussion

In recent years, the use of MRI in clinical practice for evaluating the anterior mediastinum has considerably increased due to technological improvements and characterization of

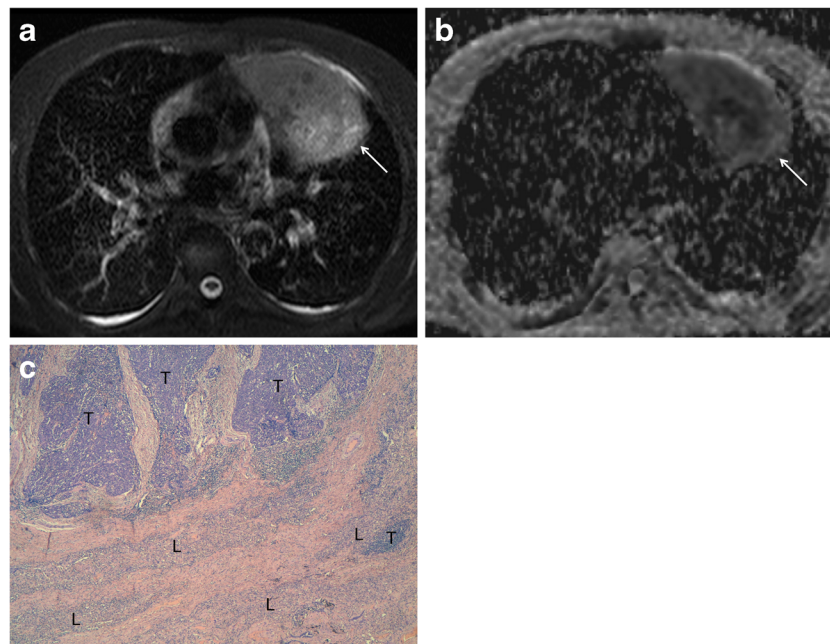


Fig. 4 High-risk and advanced thymoma in a 28-year-old woman (WHO type B3, Masaoka-Koga stage IVb for lymph node metastasis). **a** Transverse T2-weighted fat-suppressed MR image demonstrates an oval-shaped solid mass (arrow; maximal diameter, 91 mm) in the anterior mediastinum, adjacent to the pulmonary trunk, with intermediate and high signal intensity. **b** The ADC-map of DW-MRI demonstrates heterogeneous dark appearance of the mass (arrow), lower than that of muscles, with a mean ADC of 1.006×10^{-3} mm²/sec

(standard deviation, 0.235; minimum and maximum value, 0.190 and 1.457×10^{-3} mm²/sec, respectively). **c** Photomicrograph of a representative histological section shows islands of thymoma (T) composed of a prominent population of epithelial cells mixed with a minor component of lymphocytes. Tumour cells are closely adjacent or interspersed with lung cells (L), consistent with lung invasion (haematoxylin and eosin stain, original magnification $\times 40$)

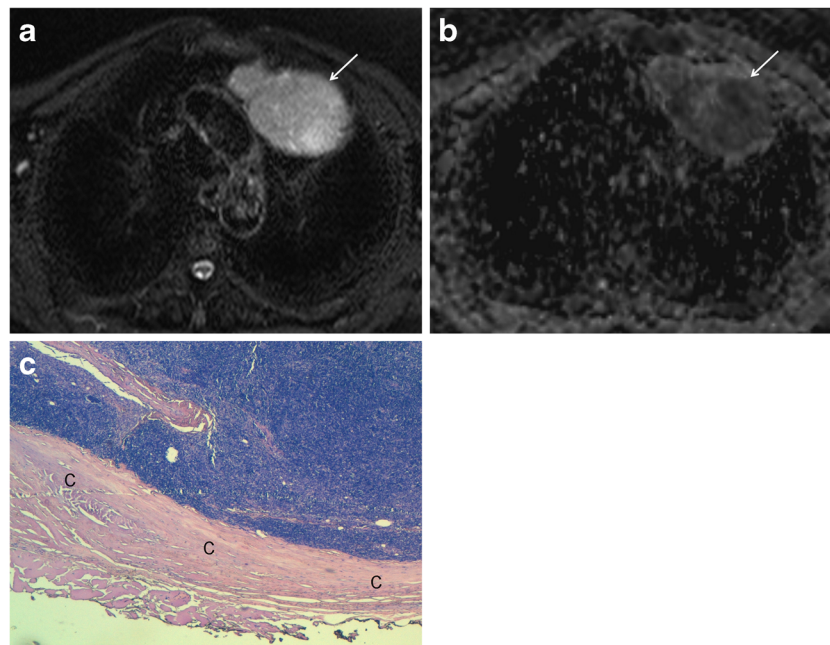


Fig. 5 High-risk and early thymoma in a 50-year-old man (WHO type B2, Masaoka-Koga stage IIb). **a** Axial T2-weighted fat-suppressed MR image detects an oval-shaped unilateral soft tissue mass (*arrow*; maximal diameter, 74 mm), adjacent to the aortic arch, with lobulated margins and slightly heterogeneous high signal intensity. **b** The ADC-map of DW-MRI demonstrates heterogeneous dark appearance of the mass (*arrow*) with a mean ADC of $1.175 \times 10^{-3} \text{ mm}^2/\text{sec}$ (standard deviation, 0.289; minimum and maximum value, 0.289 and $2.072 \times 10^{-3} \text{ mm}^2/\text{sec}$,

respectively). **c** Photomicrograph of a representative histological section shows a tissue of high cellular density characterized by mixed composition of lymphocytes and predominant epithelial cells resembling the normal thymic cortex. The tumour is completely encapsulated (C, capsule) and microscopic areas of tumour cells are appreciable into the thick capsule (haematoxylin and eosin stain, original magnification $\times 40$)

tumours; even characterization by means of quantitative data has become possible [19, 26–30]. For DW-MRI, our research demonstrates that quantitative assessment of thymomas is helpful in differentiating low-risk from high-risk tumours and the more aggressive type-B3 from all other histological types according to WHO classification, including type-B2,

being that the ADC of type-B3 and high-risk thymomas is significantly lower compared with the other defined groups. This finding reflects the ability of DW-MRI in differentiating thymomas based on their different histological composition because lower ADC values are expected for type-B3 thymomas which are typically characterized by a prominent

Table 7 Details of patients with disease recurrence during the observational period

Patient sex, age	Primary tumour		ADC*	Time to recurrence [§]	Site of recurrence	Treatment for recurrence [#]	Final outcome
	WHO	Masaoka					
F, 55	B2	II	1.299	12	Local	SR/RT	Alive (60)
M, 42	B3	III	0.728	22	Regional	SR	Alive (50)
F, 59	B3	III	1.201	12	Local	SR	Alive (28)
M, 66	B2	III	1.194	14	Regional	CT/RT	Alive (44)
M, 46	B1	III	1.499	50	Regional	SR	Alive (66)
F, 38	B3	IV	0.981	51	Regional	CT/RT	Alive (72)
M, 71	B3	II	1.153	36	Local	SR	Alive (58)

* $\times 10^{-3} \text{ mm}^2 \text{ s}^{-1}$.

[§] Interval from surgery to recurrence detection during observational period in months.

Site of recurrence: Local = recurrent disease in the anterior mediastinum or lower neck, or contiguous to the initial thymoma; Regional = intrathoracic recurrent disease in the pleura (visceral or parietal) or pericardium not contiguous with the thymus bed.

[#] RT = radiation therapy; CT = chemotherapy; SR = surgical resection.

Numbers in parentheses (column “final outcome”) are months from diagnosis to last follow-up.

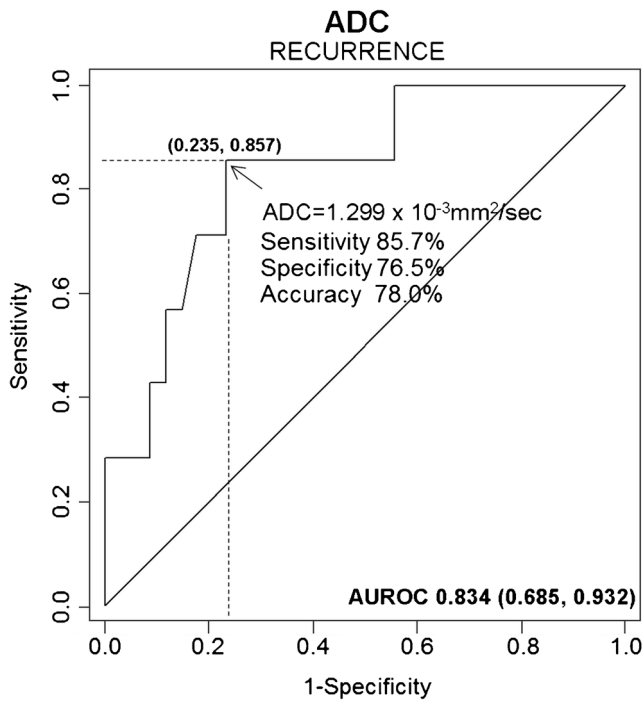


Fig. 6 Receiver operating characteristic (ROC) curve shows the sensitivity, specificity, and diagnostic accuracy of ADC-based differentiation in the prediction of recurrence. The optimal cut-point value is reported with the relative values of sensitivity, specificity, and diagnostic accuracy

population of medium-sized polygonal epithelial cells and are the only histological type of thymoma that presents nuclear atypia and prominent nucleoli [7]. Indeed, in our study, diagnostic performance of DW-MRI was greater for distinguishing type B3 from all other histological types of thymoma rather than for differentiating high-risk from low-risk thymomas, demonstrating a closer correlation with the simplified WHO classification proposed by Rieker et al. (which consists of

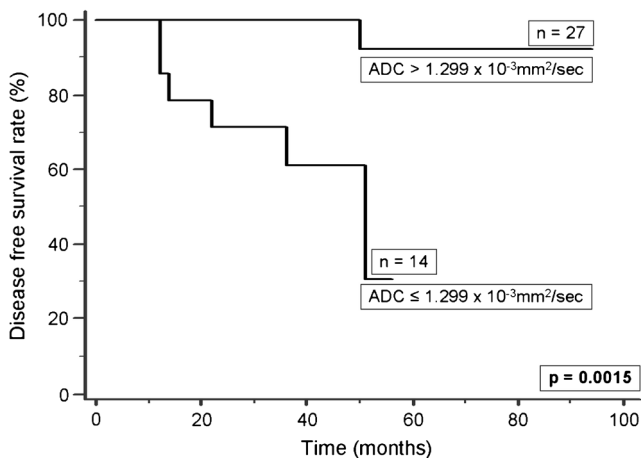


Fig. 7 Kaplan-Meier curves show a comparison of disease-free survival between groups of patients with ADC of the primary tumour higher ($n=27$) and lower or equal ($n=14$) than the optimal threshold value of $1.299 \times 10^{-3} \text{ mm}^2/\text{sec}$ for the prediction of recurrence

Table 8 Univariate analysis of clinicopathological factors and imaging parameters for DFS

Factor	No. of patients	DFS rate (%)	<i>p</i>
Gender			
Male	19	78.9	0.603
Female	22	86.3	
Age (years)			
≤55	16	75.0	0.349
>55	25	88.0	
Size (mm)			
≤52	29	58.3	0.007
>52	12	93.1	
WHO*			
Low-risk	19	94.7	0.052
High-risk	22	72.7	
Masaoka-Koga			
Early	24	91.7	0.144
Advanced	17	70.6	
Resection status			
R0	36	86.1	0.041
R+	5	60.0	
ADC ($\times 10^{-3} \text{ mm}^2/\text{sec}$)			
≤1.299	14	57.1	0.001
>1.299	27	96.3	

* Jeong simplification of WHO classification [9].

types A-AB-B1-B2 as one group and type-B3 as an other group) compared with the Jeong classification [9, 31].

For DW-MRI, there is a lack of standardization for analyzing tissue ADCs among different studies, first in the acquisition parameters (e.g., echo time, number and amplitude of *b* values) and image analysis, which makes it not possible to compare quantitative data among studies and to deduce optimal thresholds to use for characterizing thymomas in clinical practice [14–19]. Indeed, Abdel Razek et al. have found different mean ADC values for each type of tumour according to WHO classification, a lower optimal cut-point of $1.235 \times 10^{-3} \text{ mm}^2/\text{sec}$ for discriminating high-risk from low-risk TETs, and a lower AUROC of 0.804, compared with our results [19]. This discordance may be due to different technical parameters in acquisition and analysis of DW-MRI for obtaining ADC measurements among such studies, which may have influenced the ADC value. First, although echo time should be kept as short as possible (typically 50–65 msec in thoracic MRI for avoiding underestimation of ADC measurements), the unusual choice of a long echo time of 108 msec by Abdel Razek et al. (used two *b* values of 0 and $1000 \text{ sec}/\text{mm}^2$) led to a reduction in ADC which was higher for tissues with higher diffusion restriction, such as high-risk thymomas and thymic carcinomas [19, 32–35]. Indeed, the underestimation of the ADC is up to 30 % by using two *b* values of 100 and

1000 sec/mm² and an echo time of 92 msec compared with ADC measurements obtained with similar b values and an echo time of 52 msec [32]. Moreover, ADC measurements obtained by Abdel Razek et al. were also influenced by inclusion of a b value of 0 sec/mm² for ADC computation, which led to “perfusion-bias” with greater overestimation in measurements for higher vascular tissues, such as type-B3 thymoma and thymic carcinoma [19]. Indeed, because low b values are able to detect water molecules with a large degree of motion or great diffusion distance and because blood flow is completely suppressed at a b value of 150 sec/mm², the b value of 0 s/mm² should be always excluded from ADC computation to separately assess the effects of perfusion and diffusion in order to enable calculation of perfusion-insensitive ADC measurements [23]. Hence, in quantitative DW-MRI, standardization of acquisition parameters and data analysis is needed for obtaining reproducible ADC measurements and reliable optimal cut-off points.

Conversely to WHO classification, in our study, DW-MRI did not show the excellent predictive ability for distinguishing early from advanced disease according to the Masaoka-Koga system. Although mean ADC was significantly different between groups per univariate analysis, such significance was not confirmed neither via two-way ANOVA analysis nor via an adjusted logistic regression model, suggesting the inability of DW-MRI in predicting the invasiveness of thymomas regardless of their histological type. This finding is confirmed by the insignificant differences in mean ADC values of a specific WHO histological type of thymoma between cases grouped in the early and advanced disease that we found in our study. The ability of DW-MRI in predicting early or advanced disease strongly depends on the degree of association between Jeong and Masaoka-Koga classifications in the study cohort. For example, in the study of Abdel Razek et al., in which the ADC was able to discriminate among early and advanced disease ($p=0.005$), the strong correlation between classifications is suggested by the low percentage of high-risk thymomas in the early-disease group (2/9 patients, 22 %), whereas this percentage is higher in previous clinical studies and in our cohort (8/22 subjects, 36 %) [10, 19]. Furthermore, Abdel Razek et al. included in the advanced-disease group five thymic carcinomas (31 % of tumours defined as advanced disease), but none in the early-disease group [19]. Because thymic carcinomas are typically characterized by low ADC values, their inclusion in the advanced-disease group leads to a reduction of mean ADC value of such group compared with the early-disease group, promoting a finding of statistical significance. Thus, thymic carcinomas should be grouped separately because they have different histology compared with thymomas, exhibit an aggressive behaviour and occasionally are classified as early-stage disease [36].

Considering prognosis, we found a significant difference for DFS between subjects divided by an ADC cut-point value of 1.299×10^{-3} mm²/sec, DFS being poorer in patients with low ADC compared with patients with high ADC. Moreover, ADC obtained prior to treatment was a significant predictor and independent prognostic parameter of DFS for thymoma in our study population, confirming a greater risk of recurrence for patients with ADC lower than the threshold value. Similar results were obtained in studies which evaluated the prognostic value of ADC in different tumours other than thymoma [37–39]. Hence, ADC has significant impact on recurrence and should be considered to have, even for thymoma, prognostic value on DFS in addition to existing quantitative imaging parameters such as SUV_{max} [40, 41]. Thus, DW-MRI is helpful in stratification of risk and could be used for optimizing clinical decision-making at time of diagnosis.

The present study has some limitations. First, although this was the largest series of thymomas investigated with DW-MRI, the sample size was limited to a small number of patients. However, the only research which has solely investigated TETs included mixed populations of patients with thymic carcinoma and thymoma, creating difficulties in the applicability of cut-point ADC values in the general population for their daily clinical use [19]. Second, our proposed cut-points were derived from the data analyzed and require validation in independent samples of patients before being recommended for use in clinical practice. Third, the duration of follow-up was relatively short for our patients with thymoma, which typically has higher DFS and overall-survival rates compared with the highly aggressive thymic carcinoma which was excluded from this study.

In conclusion, the ADC of DW-MRI was shown to be highly reproducible and accurate quantitative parameter for distinguishing high-risk from low-risk thymomas and the more aggressive type-B3 thymoma from all other histological types according to WHO classification. Conversely, the ability of DW-MRI in determining stage based on the Masaoka-Koga system is uncertain, depends on the degree of correlation among WHO and Masaoka-Koga classifications in the study cohort, and requires further validations. Lastly, the ADC of a primary tumour has prognostic value on DFS after surgical resection of thymomas and could be used to predict recurrence, thereby improving disease stratification and guiding the treatment strategy for each patient.

Acknowledgments The scientific guarantor of this publication is Adriano M. Priola. The authors of this manuscript declare no relationships with any companies whose products or services may be related to the subject matter of the article. The authors state that this work has not received any funding. One of the authors (Maria T. Giraudo) has significant statistical expertise. Institutional review board approval was obtained. Written informed consent was obtained from all subjects (patients) in this study. Methodology: prospective, observational/diagnostic or prognostic study, performed at one institution.

References

- Priola AM, Priola SM, Cardinale L, Cataldi A, Fava C (2006) The anterior mediastinum: diseases. *Radiol Med* 111:312–342
- Wright CD (2008) Management of thymomas. *Crit Rev Oncol Hematol* 65:109–120
- Nishino M, Ashiku SK, Kocher ON, Thurer RL, Boiselle PM, Hatabu H (2006) The thymus: a comprehensive review. *Radiographics* 26:335–348
- Henschke CI, Lee IJ, Wu N et al (2006) CT screening for lung cancer: prevalence and incidence of mediastinal masses. *Radiology* 239:586–590
- Novello S, Fava C, Borasio P et al (2005) Three-year findings of an early lung cancer detection feasibility study with low-dose spiral computed tomography in heavy smokers. *Ann Oncol* 16:1662–1666
- Priola AM, Priola SM, Giaj-Levra M et al (2013) Clinical implications and added costs of incidental findings in an early detection study of lung cancer by using low-dose spiral computed tomography. *Clin Lung Cancer* 14:139–148
- Müller-Hermelink HK, Ströbel P, Zettl A et al (2004) Combined thymic epithelial tumours. In: Travis WD, Brambilla E, Müller-Hermelink HK, Harris CC (eds) *Pathology and genetics of tumours of the lung, pleura, thymus and heart (WHO classification of tumours series)*. IARC Press, Lyon, pp 196–198
- Masaoka A, Monden Y, Nakahara K, Tanioka T (1981) Follow-up study of thymomas with special reference to their clinical stages. *Cancer* 48:2485–2492
- Jeong YJ, Lee KS, Kim J, Shim YM, Han J, Kwon OJ (2004) Does CT of thymic epithelial tumors enable us to differentiate histologic subtypes and predict prognosis? *AJR Am J Roentgenol* 183:283–289
- Okuma Y, Hosomi Y, Watanabe K et al (2014) Clinicopathological analysis of thymic malignancies with a consistent retrospective database in a single institution: from Tokyo Metropolitan Cancer Center. *BMC Cancer* 14:349–357
- Priola AM, Priola SM (2014) Imaging of thymus in myasthenia gravis: from thymic hyperplasia to thymic tumor. *Clin Radiol* 69:e230–e245
- Landwehr P, Schulte O, Lackner K (1999) MR imaging of the chest: mediastinum and chest wall. *Eur Radiol* 9:1737–1744
- Priola SM, Priola AM, Cardinale L, Perotto F, Fava C (2006) The anterior mediastinum: anatomy and imaging procedures. *Radiol Med* 111:295–311
- Shin KE, Yi CA, Kim TS et al (2014) Diffusion-weighted MRI for distinguishing non-neoplastic cysts from solid masses in the mediastinum: problem-solving in mediastinal masses of indeterminate internal characteristics on CT. *Eur Radiol* 24:677–684
- Gümüştaş S, Inan N, Sarisooy HT (2011) Malignant versus benign mediastinal lesions: quantitative assessment with diffusion weighted MR imaging. *Eur Radiol* 21:2255–2260
- Abdel Razek A, Soliman N, Elashery R (2012) Apparent diffusion coefficient values of mediastinal masses in children. *Eur J Radiol* 81:1311–1314
- Abdel Razek A, Elmorsy A, Elshafey M, Elhadey T, Hamza O (2009) Assessment of mediastinal tumors with diffusion weighted single shot echo planar MR imaging. *J Magn Reson Imaging* 30:535–540
- Seki S, Koyama H, Ohno Y et al (2014) Diffusion-weighted MR imaging vs. multi-detector row-CT: direct comparison of capability for assessment of management needs for anterior mediastinal solitary tumors. *Eur J Radiol* 83:835–842
- Abdel Razek AA, Khairy M, Nada N (2015) Diffusion-weighted MR imaging in thymic epithelial tumors: correlation with World Health Organization classification and clinical staging. *Radiology* 273:268–275
- Priola AM, Priola SM (2015) Usefulness of diffusion-weighted MR imaging in predicting Masaoka-Koga clinical staging of thymic epithelial tumors by using the apparent diffusion coefficient. *Radiology* 274:936–937
- Filli L, Wumig MC, Luechinger R, Eberhardt C, Guggenberger R, Boss A (2015) Whole-body intravoxel incoherent motion imaging. *Eur Radiol*. doi:10.1007/s00330-014-3577-z
- Zhang YD, Wang Q, Wu CJ (2015) The histogram analysis of diffusion-weighted intravoxel incoherent motion (IVIM) imaging for differentiating the gleason grade of prostate cancer. *Eur Radiol* 25:994–1004
- Padhani AR, Guoying L, Mu-Koh D et al (2009) Diffusion-weighted magnetic resonance imaging as a cancer biomarker: consensus and recommendations. *Neoplasia* 11:102–125
- Koh DM, Collins DJ (2007) Diffusion-weighted MRI in the body: applications and challenges in oncology. *AJR Am J Roentgenol* 188:1622–1635
- Priola AM, Priola SM (2013) Influence of selected b values on ADC quantification in diffusion-weighted MRI. Comment on Punwani et al.: Diffusion-weighted MRI of lymphoma: prognostic utility and implications for PET/MRI? *Eur J Nucl Med Mol Imaging* 40:1108–1809
- Priola AM, Priola SM, Giraudo MT et al (2015) Chemical-shift and diffusion-weighted magnetic resonance imaging of thymus in myasthenia gravis: usefulness of quantitative assessment. *Investig Radiol* 50:228–238
- Priola AM, Priola SM, Ciccone G et al (2015) Differentiation of rebound and lymphoid thymic hyperplasia from anterior mediastinal tumors with dual-echo chemical-shift magnetic resonance imaging in adulthood: reliability of the chemical-shift ratio and signal-intensity index. *Radiology* 274:238–249
- Inchingolo R, De Gaetano AM, Curione D et al (2015) Role of diffusion-weighted imaging, apparent diffusion coefficient and correlation with hepatobiliary phase findings in the differentiation of hepatocellular carcinoma from dysplastic nodules in cirrhotic liver. *Eur Radiol* 25:1087–1096
- Fischer MA, Nanz D, Hany T et al (2011) Diagnostic accuracy of whole-body MRI/DWI image fusion for detection of malignant tumours: a comparison with PET/CT. *Eur Radiol* 21:246–255
- Priola AM, Galetto G, Priola SM (2014) Diagnostic and functional imaging of thymic and mediastinal involvement in lymphoproliferative disorders. *Clin Imaging* 38:771–784
- Rieker RJ, Hoegel J, Morresi-Hauf A et al (2002) Histologic classification of thymic epithelial tumors: comparison of established classification schemes. *Int J Cancer* 98:900–906
- Schmidt H, Gatidis S, Schwenzer NF, Martirosian P (2015) Impact of measurement parameters on apparent diffusion coefficient quantification in diffusion-weighted-magnetic resonance imaging. *Investig Radiol* 50:46–56
- Ackman JB (2014) A practical guide to nonvascular thoracic magnetic resonance imaging. *J Thorac Imaging* 29:17–29
- Abdel Razek AAK (2012) Diffusion magnetic resonance imaging of chest tumors. *Cancer Imaging* 12:452–463
- Padhani AR, Koh DM, Collins DJ (2011) Whole-body diffusion-weighted MR imaging in cancer: current status and research directions. *Radiology* 261:700–718
- Roden AC, Yi ES, Cassivi SD, Jenkins SM, Garces YI, Aubry MC (2013) Clinicopathological features of thymic carcinomas and the impact of histopathological agreement on prognostical studies. *Eur J Cardiothorac Surg* 43:1131–1139
- Hatakenaka M, Nakamura K, Yabuuchi U et al (2014) Apparent diffusion coefficient is a prognostic factor of head and neck

- squamous cell carcinoma treated with radiotherapy. *Jpn J Radiol* 32: 80–89
38. Giganti F, Orsenigo E, Esposito A et al (2015) Prognostic role of diffusion-weighted MR imaging for resectable gastric cancer. *Radiology*. doi:[10.1148/radiol.15141900](https://doi.org/10.1148/radiol.15141900)
 39. Nakamura K, Joja I, Nagasaka T et al (2012) The mean apparent diffusion coefficient value (ADC_{mean}) on primary cervical cancer is a predictive marker for disease recurrence. *Gynecol Oncol* 127: 478–483
 40. Seki N, Sakamoto S, Karube Y, Oyaizu T, Ishihama H, Chida M (2014) ¹⁸F-fluorodeoxyglucose positron emission tomography for evaluation of thymic epithelial tumors: utility for World Health Organization classification and predicting recurrence-free survival. *Ann Nucl Med* 28:257–262
 41. Kaira K, Murakami H, Miura S et al (2011) ¹⁸F-FDG uptake on PET helps predict outcome and response after treatment in unresectable thymic epithelial tumors. *Ann Nucl Med* 25: 247–253